J. Solids Structures, 1965, Vol. 1, pp. 243 to 255. Pergamon Press Ltd. Printed in Great Britain

PLASTIC TORSION OF A RECTANGULAR BAR WITH JUMP NON-HOMOGENEITY

J. RYCHLEWSKI

Institute of Fundamental Technical Problems, Warsaw, Poland

Abstract—The problems of plastic jump non-homogeneity, i.e. the problems concerned with a jump-like change of the yield limit, were considered in previous papers by the author. In the present work, a rectangular bar composed of two materials with different yield limits and subjected to torsion is considered. It turns out that even for such a simple problem nine different solutions exist depending on the values of three parameters characterizing non-homogeneity, form, and partition of the cross-section.

THE problem of purely plastic torsion of homogeneous bars has been well explored (cf. for instance, [1]). Reference [2] contains an analysis of torsion of non-homogeneous bars with continuous distribution of the yield limit.

In applications we have often to do with bars composed of several different materials. The problem of limit load of such bars reduces to the necessity of considering the case where the yield limit undergoes a jump change on certain lines. Such a non-homogeneity has been called in [3] a jump non-homogeneity.

Reference [4] contains a general analysis of the problem of plastic torsion for a jump non-homogeneity, the properties of the stress field in the neighbourhood of a contact line, an analysis of the form of solution in the neighbourhood of the intersection of the contact line and the edge (local solution), a discussion of Nadai's analogies and a solution example for a circular bar. Homogeneous bars of multiply connected cross-section constitute a particular case of the class of bar studied in [4].

Let us consider here the bar with cross-section as shown in Fig. 1. The rectangle $2a \times 2b$ is divided by the contact line L normal to the edge $2b$ into two regions G_-, G_+, whose widths are c and $2b-c$, respectively. The materials in the regions G_-, G_+ have constant but different yield limits K_-, K_+, $K_+ > K_-$. The strength of the joint is characterized by a third number K_0 equal to the maximum shear stress that can be transferred across the contact surface.

It will be assumed that the adhesion is perfect, that is

$$K_0 \geqslant K_-, \tag{1}$$

which excludes the quantity K_0 from further considerations (cf. [3, 4]).

The problem is characterized by three independent parameters, for instance

$$0 \leqslant \lambda = \frac{K_-}{K_+} \leqslant 1, \qquad 0 \leqslant \frac{a}{b} \leqslant \infty, \qquad 0 \leqslant \frac{c}{b} \leqslant 2. \tag{2}$$

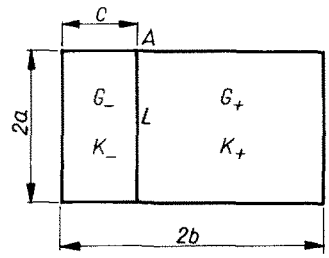

FIG. 1.

They may be called parameters of non-homogeneity, form and partition, respectively. The components of the vector of shear stress

$$\vec{\tau} = \tau_{xz}\vec{l}_x + \tau_{yz}\vec{l}_y \tag{3}$$

must satisfy the equilibrium equation

$$\tau_{xz,x} + \tau_{yz,y} = 0, \tag{4}$$

the yield condition

$$|\vec{\tau}|^2 = \tau_{xz}^2 + \tau_{yz}^2 = \begin{cases} K_-^2 & \text{in } G_-, \\ K_+^2 & \text{in } G_+, \end{cases} \tag{5}$$

and the boundary condition $\tau_{tz} = 0$ at the contour.

The continuity condition of the normal component

$$\vec{\tau}_+ \cdot \vec{n} = \vec{\tau}_- \cdot \vec{n} \tag{6}$$

must be satisfied on the contact line L, where $\vec{n}$ is the unit vector normal to L. On the contact line we have therefore a discontinuity of stress. The vector of shear stress undergoes a rotation.

On introducing the stress function by means of the classical equations

$$\tau_{xz} = F_{,y}, \qquad \tau_{yz} = -F_{,x}, \tag{7}$$

we satisfy (4) identically. From the condition (5) we have

$$|\text{grad } F| = \begin{cases} K_- & \text{in } G_-, \\ K_+ & \text{in } G_+. \end{cases} \tag{8}$$

The problem of finding the stresses satisfying (4), (5) is therefore equivalent to the construction of a continuous surface $F(x, y)$ with constant slope, different in G_- and G_+. It should be stressed that neither of the two problems has a unique solution. From the set of solutions we must select that which is in agreement with the kinematic conditions. If these are not considered the correct solution is, according to the extremum theorems of plasticity, that corresponding to the highest value of the limiting twisting moment,

$$M = 2 \iint_{G_- + G_+} F \, dx \, dy. \tag{9}$$

Let us proceed to obtain the local solution in the neighbourhood of point A, the set of coordinates assumed being that of Fig. 2.

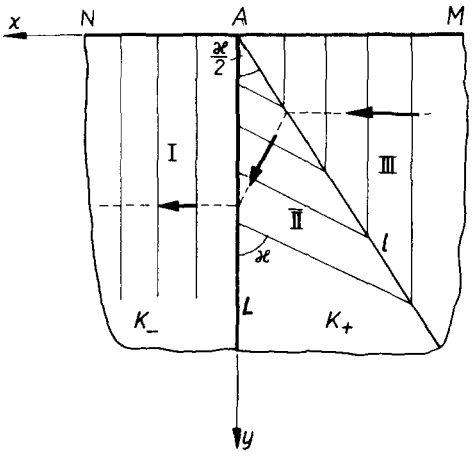

FIG. 2.

In the neighbourhood of the edge AN of the weaker material (region I) the solution of the equation (4), (5) has the form

$$\tau_{xz}^{I} = K_-, \qquad \tau_{yz}^{I} \equiv 0. \tag{10}$$

The continuity condition (6) must be satisfied at the contact line L, that is $\tau_{xz}^{-} = \tau_{xz}^{+}$. Therefore the solution in the stronger material has in the neighbourhood of L (region II), the form

$$\tau_{xz}^{II} = K_+ \cos \varkappa, \qquad \tau_{yz}^{II} = K_+ \sin \varkappa. \tag{11}$$

The vector $\vec{\tau}^{II}$ (whose modulus is K_+) is rotated in relation to $\vec{\tau}^{I}$ (whose modulus is K_-) through the angle

$$\varkappa = \arccos \frac{K_-}{K_+}, \qquad 0 \leqslant \varkappa \leqslant \frac{\pi}{2}.$$

In the neighbourhood of the edge of the stronger material (region III) the solution has the form

$$\tau_{xz}^{III} = K_+, \qquad \tau_{yz}^{III} \equiv 0. \tag{12}$$

Starting from the intersection point of the contact line L with the edge of the cross-section a discontinuity line l penetrates into the stronger region. Its form can be obtained from the condition $\vec{\tau}^{III} \cdot \vec{n} = \tau^{II} \cdot \vec{n}$. We have

$$l: \quad y = -\cot \varkappa/2 \cdot x.$$

Figure 2 shows the slip lines which are orthogonal at every point to $\vec{\tau}$ and a trajectory of the vector $\vec{\tau}$. The surface $F(x, y)$ is composed, in the neighbourhood of A, of three plane sheets.

Depending on the properties of the parameters λ, a/b, c/b, the problem of limit load of the bar has nine different solutions.

*Solution 1, Figure 3**

From the corner N a discontinuity line l_1 propagates thus dividing the weaker zone into the regions I, II in which the slip-lines are normal to NA and NS, respectively. In view of the maximum condition of the limit moment it is assumed that there are no other discontinuity lines in the weaker region and that l_1 intersects the contact line at a point A_{10}. In the neighbourhood of A the image is that of Fig. 2. The discontinuity line l_2 is inclined to L at an angle $\varkappa/2$. In region III the slip lines are parallel and inclined at an angle $\varkappa$ to L. On the sector $A_{10}B$ of the line L the vector τ^- is parallel to L, therefore $\vec{\tau}^+$ is also parallel (cf. Fig. 3) therefore the slip lines in the region IV are normal to $A_{10}B$. A discontinuity line l_3 passes through A_{10}, bisecting the angle between the slip lines of the regions III and IV. The slip lines l_2, l_3 have an intersection point A_{23}. Since in the region V the slip lines are normal to the edge AM and in the region IV they are normal to $A_{10}B$, a discontinuity line l_4 therefore passes through A_{23} at an angle $\pi/4$ to these lines. It intersects the symmetry axis at A_{4s}. The discontinuity lines l_5, l_6 require no comment.

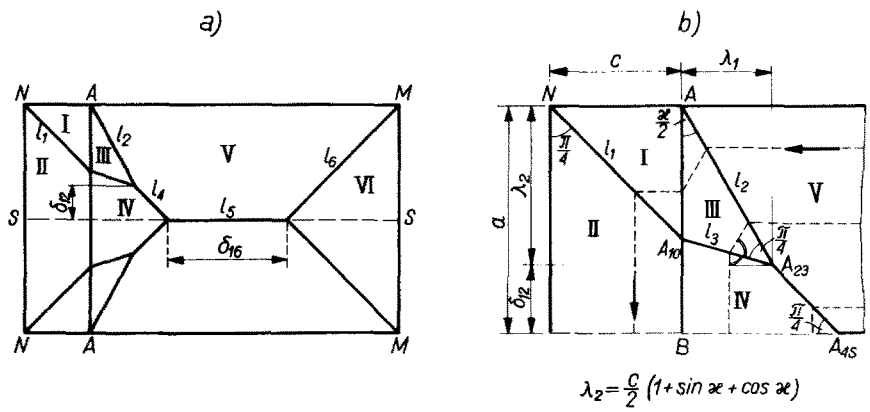

FIG. 3.

The characteristic dimensions and angles can easily be determined on the basis of this analysis. They are given in Fig. 3(b).

The stress surface F is composed of plane sheets† different in each region. The discontinuity lines $l_i (i = 1, \ldots 6)$ are segments of projections of straight lines constituting the intersections of the sheets of F. Sufficient information on the surface F is furnished by the ordinates of the points A_{10}, A_{23}, A_{4s},

$$F_{10} = K_+ c \cos\varkappa, \qquad F_{23} = \tfrac{1}{2} K_+ c(1 + \sin\varkappa + \cos\varkappa), \qquad F_{4s} = K_+ a, \tag{13}$$

and the F = const. lines (Fig. 3(b)), that is the trajectories of shear stress. The function F reaches its maximum constant value on the discontinuity line l_5. The limit moment can be found from (9).

* All the figures are drawn for $\lambda = K_-/K_+ = 0{,}5$, $\varkappa = 60°$.

† In the problem considered we shall be concerned only with regions of parallel slip lines (plane sheets of F); therefore this will no longer be mentioned.

If c is small in relation to a, b, the set of discontinuity lines l_1, l_2, l_3 is comprised in a small neighbourhood of the corner N and disturbs in an insignificant manner the well-known solution for the homogeneous body.

The solution obtained is valid if the point A_{23} lies above the symmetry axis and the point A_{4s} is to the left of the point A_{6s}. By finding the appropriate distance in Fig. 3(b) we obtain the inequalities*

$$\begin{aligned} &\delta_{12} \geqslant 0, \qquad \frac{a}{b}-\frac{1}{2}(1+\sin\varkappa+\cos\varkappa)\frac{c}{b} \geqslant 0, \\ &\delta_{16} \geqslant 0, \qquad 1-\frac{a}{b}-\frac{1}{2}(1+\cos\varkappa)\frac{c}{b} \geqslant 0. \end{aligned} \tag{14}$$

On a $\lambda = \text{const.}$ plane in the C_3-space of the parameters (2) this corresponds to the region 1 between the axis a/b and the straight lines Δ_{12}, Δ_{16}, Fig. 12, intersecting at the point Λ_1, of which the coordinates are

$$\Lambda_1: \qquad \frac{a}{b}=\frac{1+\sin\varkappa+\cos\varkappa}{2+\sin\varkappa}, \qquad \frac{c}{b}=\frac{2}{2+\sin\varkappa}. \tag{15}$$

Solution 2, Figure 4

With the increasing parameter c/b, for fixed a/b and λ, the conditions (14) may no longer be satisfied. Let us consider first the case where the condition $\delta_{12} \geqslant 0$ is not satisfied. Then, the slip lines l_2, l_3 will cross the symmetry axis at the points A_{2s}, A_{3s} before they meet at A_{23}. We obtain a modification of the previous solution, Fig. 4(a). Instead of the discontinuity line l_4 we have a new discontinuity line l_7. The characteristic distances and angles are shown in Fig. 4(b). The ordinates of the stress surface F are†

$$F_{3s} = K_+ \frac{\cos\varkappa}{1-\sin\varkappa}(a-c\sin\varkappa), \qquad F_{10} < F_{3s} < F_{2s}. \tag{16}$$

Solution 2 takes place if the distance between the points A_{2s}, A_{6s} is greater than zero, the point A_{10} lies above the symmetry axis and the distance between the points A_{3s}, A_{2s} is greater than zero. By calculating, on the basis of Fig. 4, the quantities required, we

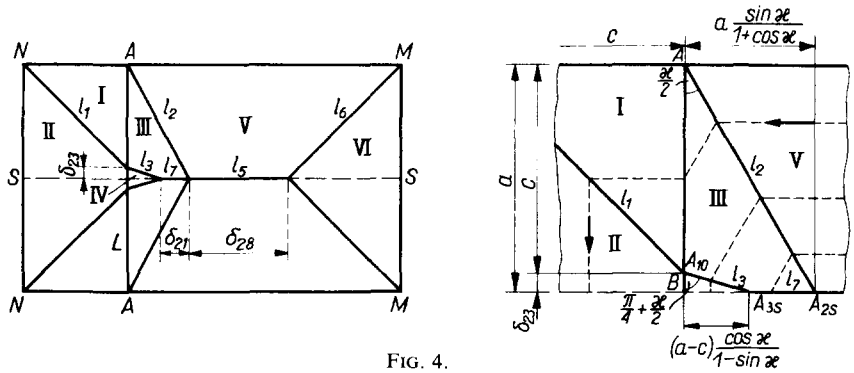

FIG. 4.

* The quantities $\delta_{\nu\mu}$ are selected so that a change of sign of $\delta_{\nu\mu}$ corresponds to a passage from the νth to the μth solution. In general $\delta_{\nu\mu} \neq \delta_{\mu\nu}$.

† We shall quote a few values only. The values of F_{ki} are the same for all the solutions in which the point A_{ki} is involved.

obtain the following inequalities

$$\delta_{21} \geqslant 0, \qquad \frac{a}{b}-\frac{1}{2}(1+\sin\varkappa+\cos\varkappa)\frac{c}{b} \leqslant 0,$$

$$\delta_{23} \geqslant 0, \qquad \frac{a}{b}-\frac{c}{b} \geqslant 0, \tag{17}$$

$$\delta_{28} \geqslant 0, \qquad 2-\frac{1+\sin\varkappa+\cos\varkappa}{1+\cos\varkappa}\frac{a}{b}-\frac{c}{b} \geqslant 0.$$

In a $\lambda = \text{const.}$ plane this corresponds to the region 2 between the straight lines Δ_{12}, Δ_{23}, Δ_{28}, Fig. 12. The straight lines Δ_{12}, Δ_{28} intersect, as is easily seen, at points Λ_1, coordinates are (15).

Solution 3, Figure 5

If, in the preceding solution, the width of the weaker zone has the value $c = a$, the point A_{10} lies on the symmetry axis S–S. The zone IV vanishes. For greater values of c the solution is shown in Fig. 5(a), (b). This is the simple solution. From Fig. 5(a) it follows directly that for sufficiently small values of the parameter a/b this solution is valid for any λ and in a broad range of values of c/b.

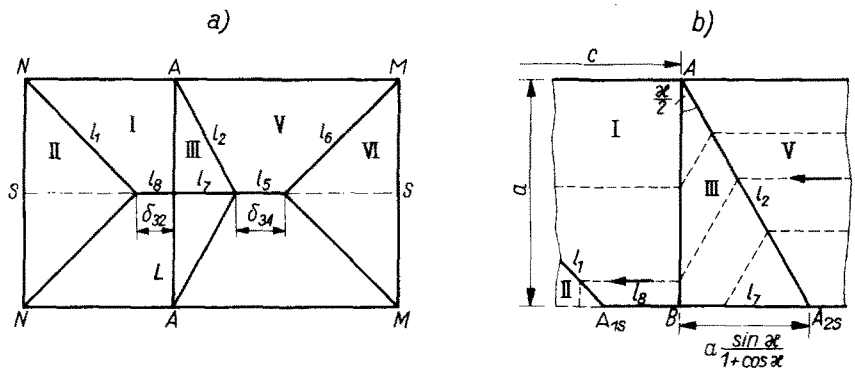

FIG. 5.

The validity region of Solution 3 is expressed by the inequalities

$$\delta_{32} \geqslant 0, \qquad \frac{a}{b}-\frac{c}{b} \leqslant 0,$$

$$\delta_{34} \geqslant 0, \qquad 2-\frac{1+\sin\varkappa+\cos\varkappa}{1+\cos\varkappa}\frac{a}{b}-\frac{c}{b} \geqslant 0. \tag{18}$$

The corresponding straight lines Δ_{23}, Δ_{34} in a $\lambda = \text{const.}$ plane have an intersection point Λ_2 whose coordinates are

$$\Lambda_2: \qquad \frac{a}{b} = \frac{c}{b} = \frac{1+\cos\varkappa}{1+\sin\varkappa+\cos\varkappa}. \tag{19}$$

Solution 4, Figure 6

With increasing parameter c/b the discontinuity lines l_2, l_6 may intersect at the point A_{26} above the symmetry axis. The point A_{26} is the origin of new discontinuity line l_9, halving the angle between the slip lines of regions III and VI.

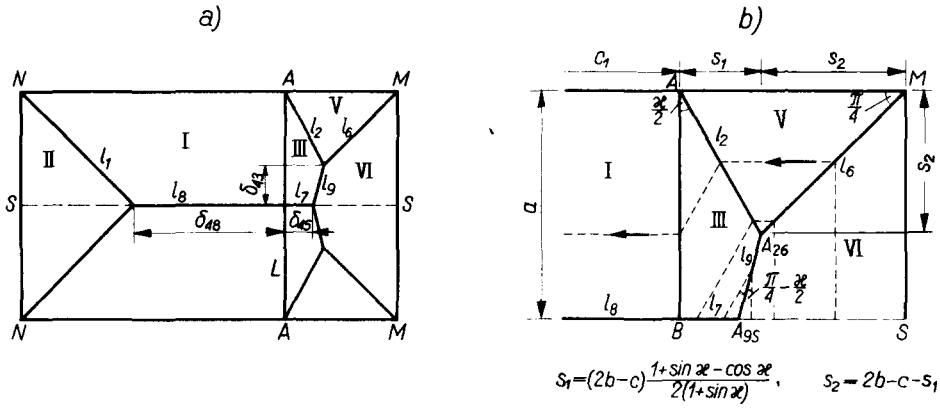

FIG. 6.

The values of the stress function F at the characteristic points are

$$F_{1s} = F_B = K_+ a\cos\varkappa, \qquad F_{9s} = K_+ \frac{a\cos\varkappa + (2b-c)\sin\varkappa}{1+\sin\varkappa},$$
$$F_{26} = K_+(2b-c)\frac{1+\cos\varkappa}{1+\sin\varkappa+\cos\varkappa}. \tag{20}$$

The greatest value of the function F (the top of the surface F) is F_{9s}. The validity range of the solution is expressed by the inequalities

$$\delta_{43} \geqslant 0, \qquad 2-\frac{1+\sin\varkappa+\cos\varkappa}{1+\cos\varkappa}\frac{a}{b}-\frac{c}{b} \leqslant 0,$$
$$\delta_{48} \geqslant 0, \qquad \frac{a}{b}-\frac{c}{b} \leqslant 0, \tag{21}$$
$$\delta_{45} \geqslant 0, \qquad \left(2-\frac{c}{b}\right)-\frac{a}{b}\cos\varkappa \geqslant 0,$$

to which correspond the straight lines Δ_{34}, Δ_{48}, Δ_{45}, Fig. 12.

Solution 5, Figure 7

Further increase of the width of the weaker zone leads to the case where the discontinuity line l_9 intersects the contact line at a point A_{90} above the symmetry axis. From the point A_{90} originates a new discontinuity line l_{10} in the weaker zone bounding a new region VII in which the slip lines are normal to the contact line L.

The values of the function F at the characteristic points are

$$F_{90} = K_+(2b-c), \qquad F_{10s} = K_+ a\cos\varkappa. \tag{22}$$

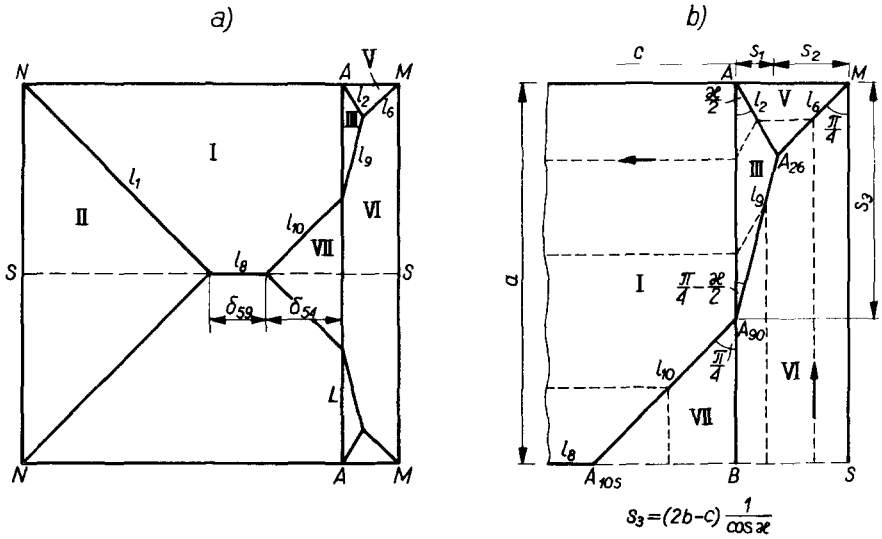

FIG. 7.

The maximum constant value is reached by the function F on the discontinuity line l_8. The validity range of Solution 5 is determined by the inequalities

$$\begin{aligned} &\delta_{54} \geqslant 0, \qquad \left(2-\frac{c}{b}\right)-\frac{a}{b}\cos\varkappa \leqslant 0, \\ &\delta_{59} \geqslant 0, \qquad \left(2-\frac{c}{b}\right)-\left(2\frac{a}{b}-\frac{c}{b}\right)\cos\varkappa \geqslant 0. \end{aligned} \tag{23}$$

The corresponding lines Δ_{45}, Δ_{59} in Fig. 12 intersect at the point Λ_3 whose coordinates are

$$\Lambda_3: \qquad \frac{a}{b}=\frac{c}{b}=\frac{2}{1+\cos\varkappa}. \tag{24}$$

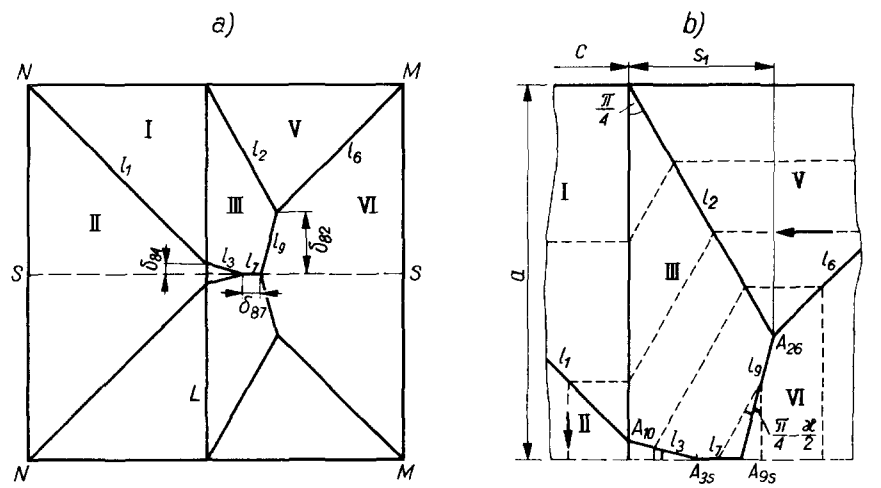

FIG. 8.

With increasing parameter c/b the inequality (23) still holding, the discontinuity lines l_2, l_6, l_9 and the corresponding zones III, V become localized in a decreasing neighbourhood of the corner M. For $c = 2b$ we obtain the solution for a homogeneous bar made of the weaker material.

Solution 8, Figure 8

Analysis of the Solutions 2,4 leads to the conclusion that there exists a narrow range of parameters, for which the discontinuity line l_3 crosses the symmetry axis and, at the same time, the discontinuity lines l_2, l_6 cross themselves above the symmetry axis. The solution is shown in Fig. 8. The stress function takes at the characteristic points the previous values. The summit of F lies above A_{9s}. The validity range of Solution 8 is expressed by the inequalities

$$\begin{aligned} &\delta_{82} \geqslant 0, \qquad 2-\frac{1+\sin\varkappa+\cos\varkappa}{1+\cos\varkappa}\frac{a}{b}-\frac{c}{b} \leqslant 0, \\ &\delta_{84} \geqslant 0, \qquad \frac{a}{b}-\frac{c}{b} \geqslant 0, \\ &\delta_{87} \geqslant 0, \qquad \left(2-\frac{c}{b}\right)\frac{\cos\varkappa}{1+\sin\varkappa}-2\frac{a}{b}+\frac{c}{b}(1+\sin\varkappa) \geqslant 0. \end{aligned} \tag{25}$$

The corresponding region in Fig. 12 is bounded by the segments Δ_{28}, Δ_{48}, Δ_{87}, constituting a triangle with its corners at Λ_1, Λ_2, Λ_3.

Solutions 6, 7, 9, Figures 9, 10, 11

It can be easily observed that the above solutions have been obtained by assuming that the ratio a/b is sufficiently small. For greater a/b we easily obtain, from the Solutions 1, 8, 5, the Solutions 6, 7, 9 shown on the respective Figs. 9, 10, 11. The characteristic

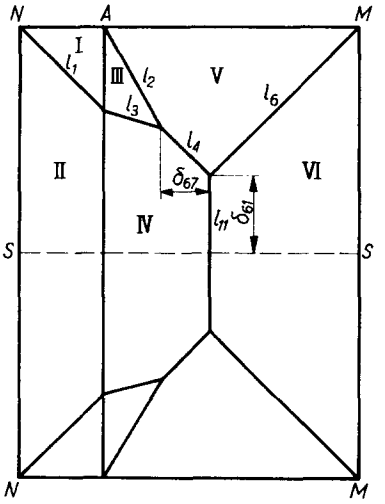

FIG. 9.

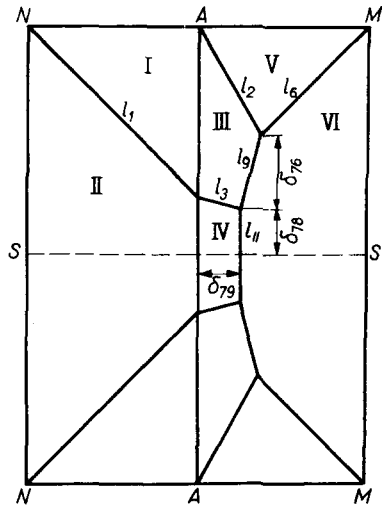

FIG. 10.

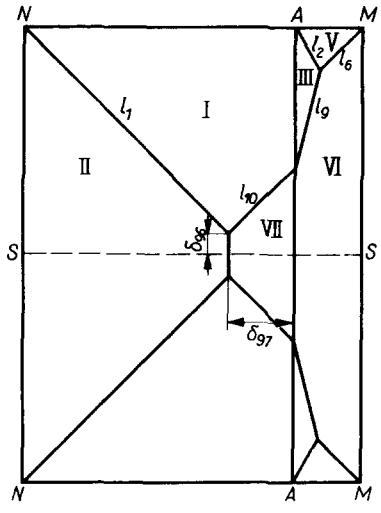

FIG. 11.

angles and dimensions and the form of the trajectories of shear stress can easily be fixed on the basis of the previous figures. The values of the stress functions at the new points A_{46} (Solution 6), A_{93} (Solution 7), $A_{1,10}$ (Solution 9) are the maximum values of the corresponding solutions,

$$F_{46} = F_{93} = F_{1,10} = K_+\left[b-\frac{c}{2}(1-\cos\varkappa)\right]. \tag{26}$$

The validity ranges are described by the following inequalities

$$\begin{aligned} &\delta_{67} \geqslant 0, \qquad \frac{c}{b} \leqslant \frac{2}{2+\sin\varkappa}, \\ &\delta_{61} \geqslant 0, \qquad 1-\frac{a}{b}-\frac{1}{2}(1+\cos\varkappa)\frac{c}{b} \leqslant 0, \end{aligned} \tag{27}$$

for Solution 6

$$\begin{aligned} &\delta_{76} \geqslant 0, \qquad \frac{c}{b} \geqslant \frac{2}{2+\sin\varkappa}, \\ &\delta_{78} \geqslant 0, \qquad \left(2-\frac{c}{b}\right)\frac{\cos\varkappa}{1+\sin\varkappa}-2\frac{a}{b}+\frac{c}{b}(1+\sin\varkappa) \leqslant 0, \\ &\delta_{79} \geqslant 0, \qquad \frac{c}{b} \leqslant \frac{2}{1+\cos\varkappa}, \end{aligned} \tag{28}$$

for Solution 7 and

$$\begin{aligned} &\delta_{97} \geqslant 0, \qquad \frac{c}{b} \geqslant \frac{2}{1+\cos\varkappa}, \\ &\delta_{95} \geqslant 0, \qquad \left(2-\frac{c}{b}\right)-\left(2\frac{a}{b}-\frac{c}{b}\right)\cos\varkappa \leqslant 0. \end{aligned} \tag{29}$$

for Solution 9.

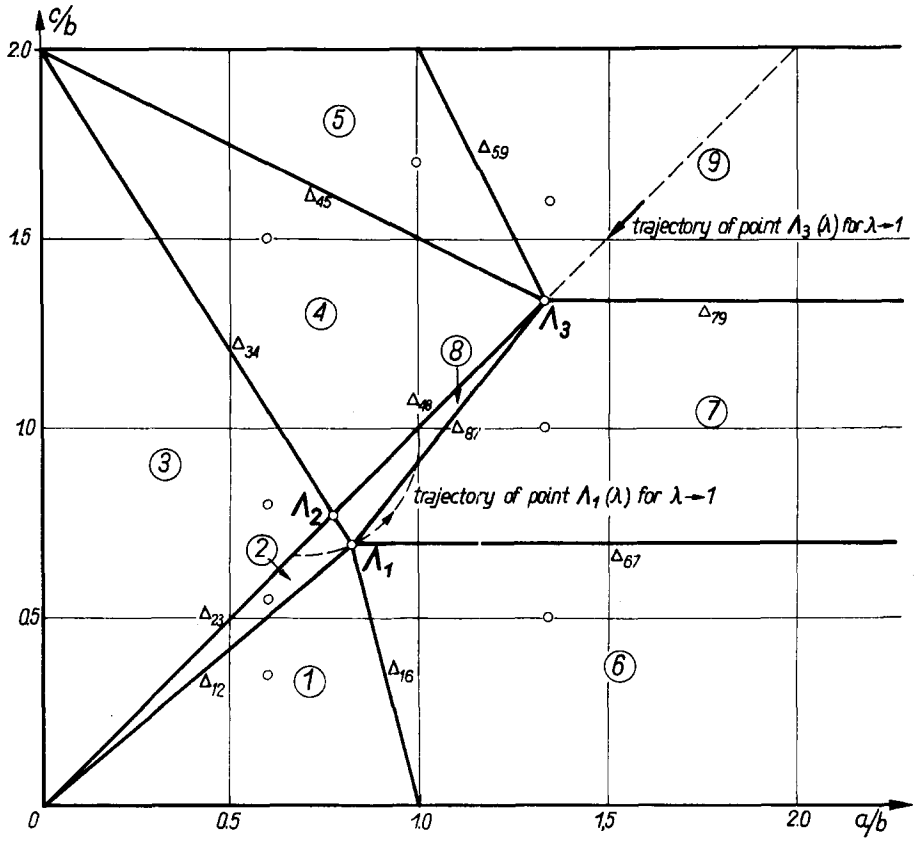

FIG. 12.

This ends the analysis of the example. The limit twisting moment for each particular solution is determined from equation (9) and the ordinates of the surface F, which requires elementary but tedious computation.

We should stress the special role of the solutions corresponding to the points Λ_1, Λ_2, Λ_3 in a $\lambda = \text{const.}$ plane whose coordinates are determined by (15), (19), (24). They have two interesting properties:

(1) From the solutions Δ_1, Λ_2, Λ_3 shown in Fig. 13 all the nine solutions can be obtained by insignificant changes of the parameters a/b, c/b.

(2) The subdivision of a $\lambda = \text{const.}$ plane into regions of applicability of each solution is determined in a unique manner by giving the points $\Lambda_1(\lambda)$, $\Lambda_3(\lambda)$. By connecting the point Λ_1 with the points $\{0,0\}$, $\{1,0\}$, $\{\infty,1\}$, Λ_3, $\{0,2\}$ we obtain the segments Δ_{12}, Δ_{16}, Δ_{67}, Δ_{78}, Δ_{28} and the location of the point Λ_2.

The influence of the value λ on the configuration of the zones $1,\ldots 9$ in a $\lambda = \text{const.}$ plane reduces therefore to a displacement of the points Λ_1, Λ_3. If $\lambda = K_-/K_+$ increases from 0 to 1 the point Λ_1 moves on the curve, whose parametric equations are (15) (dashed curve in Fig. 12) from the position $\{\frac{2}{3},\frac{2}{3}\}$ to $\{1,1\}$, and the point Λ_3 moves along the straight line $a = c$ from $\{2,2\}$ to $\{1,1\}$.

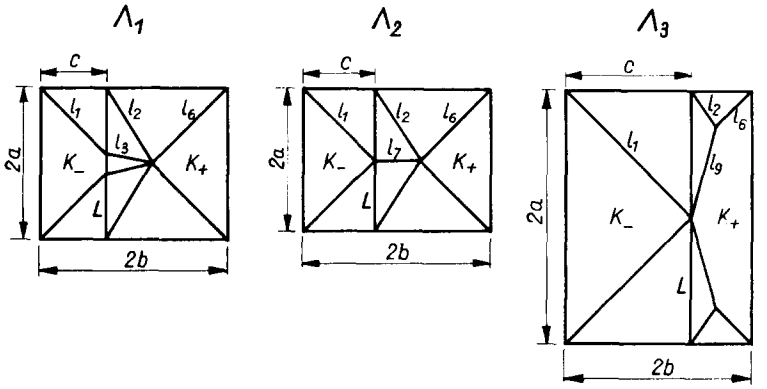

FIG. 13.

The latter circumstance simplifies considerably the use of the results obtained in practical problems. Knowing the ratio of the yield limits of the materials we obtain the location of the points Λ_1, Λ_3, draw the straight lines $\Delta_{\nu\mu}$, determine for given values of the parameters a/b, c/b the number of the solution and compute from F the limit moment.

Let us observe that the occurrence of the simplest solutions, of the type Λ_1, Λ_2, Λ_3 is generally characteristic for problems of jump non-homogeneity (cf. for instance [5]).

We can draw a number of conclusions on the classification of bars of the class just studied. Let us indicate only that

for $\frac{a}{b} < \frac{2}{3}$ we only have the solutions 1, 2, 3, 4, 5,

for $\frac{a}{b} > 2$ we only have the solutions 6, 7, 9.

The above complete solution of the problem of Fig. 1 enables us to analyse other problems of rectangular bars with jump non-homogeneity. As an example Fig. 14 shows, on the basis of the Solution 5, the form of the discontinuity lines for a bar reinforced by two symmetric inserts whose width is $c \ll a$.

The solution for a bar divided into n parts by rectangles, whose bisector lines of the apex angles coincide, Fig. 15, is trivial. The limit moment is

$$M = \frac{4}{3} \sum_{\nu=1}^{n} K_\nu [a_\nu^2(3b_\nu - a_\nu) - a_{\nu-1}^2(3b_{\nu-1} - a_{\nu-1})]. \tag{30}$$

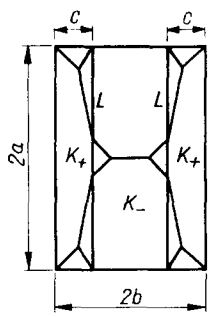

FIG. 14.

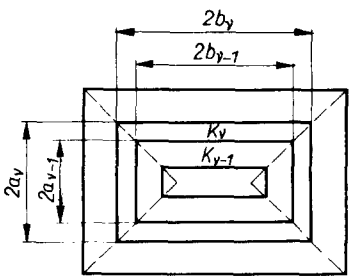

FIG. 15.

Plastic jump non-homogeneity leads to essential changes in the configuration of the slip lines and even simplest problems like that discussed above undergo surprising complications. The same can be said of the problem of plane plastic strain of bodies with jump non-homogeneity, [5, 6].

REFERENCES

[1] W. PRAGER and P. G. HODGE, *Theory of Perfectly Plastic Solids*. John Wiley, New York, London (1951).
[2] A. I. KUZNETSOV, *Arch. Mech. Stos.* **10,** 447–462 (1958).
[3] J. RYCHLEWSKI, *Bull. Acad. pol. Sci. Sér. Sci. techn.* **12,** 7 (1964).
[4] J. RYCHLEWSKI, *Acta Mechanica.* **1,** 1 (1965). In press.
[5] J. RYCHLEWSKI, *J. Mechanique.* **3,** 461 (1964).
[6] J. RYCHLEWSKI, *J. Nonlinear Mech.* **1,** 1 (1965). In press.

(*Received* 17 *August* 1964)

Zusammenfassung—Die Probleme der sprungartigen, plastischen Nichthomogenität, d.h. die Probleme, die im Zusammenhang mit einer sprungartigen Änderung der Fliessgrenze auftreten, wurden vom Verfasser in vorhergehenden Beiträgen behandelt. In der vorliegenden Arbeit wird eine rechteckige Stange untersucht, welche aus zwei Stoffen mit verschiedenen Fliessgrenzen besteht, und welche unter Torsion steht. Es stellt sich heraus, dass selbst im Falle eines derartigen einfachen Problems neun verschiedene Lösungen bestehen. Diese hängen von den Werten der drei die Nichthomogenität kennzeichnenden Parameter, von der Form und von der Querschnittsteilung ab.

Абстракт—Вопросы пластической разрывной неоднородности, т.е. вопросы пластичности тел с разрывным распределением предела текучести, рассматривались в предыдущих работах автора. В настоящей работе исследуется предельное состояние скручиваемого стержня состоящего из двух материалов с различными пределами текучести. Исследование показало, что даже этот простой пример имеет девять разных решений для разных областей значений трех параметров описывающих неоднородность, соотношение размеров сечения и его деление.